Materials Science-Poland, Vol. 24, No. 1, 2006

High-temperature phenomena in RbD_2PO_4 and CsH_2PO_4 Polymeric transformations or polymorphic phase transitions?

W. BRONOWSKA*

Institute of Physics, Wroclaw University of Technology, Wybrzeże Wyspiańskiego 27, Wrocław, Poland

X-ray analysis has been performed for RbD_2PO_4 and CsH_2PO_4 over the temperature range from 288 K to 537 K and 507 K, respectively. The refinement of the crystal structure of RbD_2PO_4 at 430 K has revealed that the high-temperature paraelectric phase of this crystal is isomorphic with the monoclinic $P2_1/m$ paraelectric phase of CsH_2PO_4. The X-ray diffraction CCD images obtained for RbD_2PO_4 have proved that the high-temperature paraelectric phase is stable up to approximately 525 K. At this temperature, polycrystallisation of the single-crystal samples and their subsequent decomposition has been observed. CsH_2PO_4 undergoes a structural phase transition at 504 K, from the monoclinic paraelectric phase to a cubic superionic phase ($P2_1/m$ transforms to $Pm\text{-}3m$ symmetry). The reversibility of the superionic phase transition in the crystals is a strong evidence for a polymorphic character of this solid–solid transition.

Key words: *X-ray analysis*; *crystal structure*; *phase transition*; *polymorphic transformation*

1. Introduction

In AH_2PO_4-type crystals (where a = K, Rb, Tl, NH_4 or Cs), two kinds of crystal systems can be stably crystallized at room temperature. The crystals of KH_2PO_4, RbH_2PO_4, and $NH_4H_2PO_4$ belong to the tetragonal system [1–3], whereas the crystals of CsH_2PO_4, TlH_2PO_4, and RbD_2PO_4 belong to the monoclinic system [1, 2, 4–8].

The RbD_2PO_4 crystal exhibits a superlattice structure with the lattice parameters a = 15.352(2) Å, b = 6,184(1) Å, c = 9.566(2) Å, β = 108,8(1)° [9], which are doubled along both the a and c axes compared to the dimensions of the unit cell of ferroelectric CsH_2PO_4 [5]. RbD_2PO_4 undergoes phase transitions at 317 K and 377 K [4]. The low-temperature phase is antiferroelectric or approximately antiferroelectric (fer-

*E-mail: wieslawa.bronowska@pwr.wroc.pl

rielectric with 2*a*, *b*, 2*c*, *Z* = 8, $P2_1$) [4]; the intermediate (non-polar, with *a*, *b*, 2*c*, *Z* = 4, $P2_1/c$, [10]) and high-temperature (*a*, *b*, *c*, *Z* = 2, $P2_1/m$ [9]) phases are paraelectric [11]. The crystal structure of the ferrielectric phase was determined at room temperature [9, 12], the structure of the intermediate phase was determined at 332 K [10]. Suzuki et al. [10] reported that the high-temperature paraelectric phase has the space group $P2_1/m$ with the basic lattice parameters, but the structure of that phase has not yet been determined.

The CsH_2PO_4 crystal exhibits ferroelectric properties below 154 K and has $P2_1$ symmetry [13, 14]. In the paraelectric phase, the crystal has $P2_1/m$ symmetry [5–8, 13, 14]. The ionic conductivity of CsH_2PO_4 undergoes a sharp increase at 504 K [15–17], from 1.2×10^{-5} to 9.0×10^{-3} $ohm^{-1}cm^{-1}$ [18].

Despite extensive studies of high-temperature transitions in MX_2PO_4 (where M = K, Rb, Cs; X = H, D) during the past few years, the microscopic nature of the high-temperature phenomena in these crystals is still not completely understood. Under normal air conditions, their ionic conductivity is related to two competing processes: a polymorphic transition and chemical decomposition with partial polymerisation. Lee [19], Ortiz et al. [16] and recently Park [20], attribute the increase of conductivity of the KDP compounds at high temperatures to the dehydration process starting on the sample surface and partial polymerisation. On the other hand, our previous powder X-ray investigations of CDP under humidified conditions [6, 7] support Baranov's et al. [15] suggestion that the superprotonic phase of CDP is cubic and reversible with hysteresis on cooling. Recently, Boysen et al. [18] and Otomo et al. [21] reconfirmed the reversibility of the superionic phase transition in these crystals.

This paper presents the results of X-ray investigations of RbD_2PO_4 and CsH_2PO_4 over the temperature range from 288 K to 537 K and 507 K, respectively. In order to explain the nature of high-temperature phenomena in these crystals, detailed structure analyses were performed using a KM4-CCD diffractometer.

2. Experimental

Single-crystal measurements of RbD_2PO_4 and CsH_2PO_4 were carried out on a four circle X-ray KM4 diffractometer (Kuma Diffraction Company) equipped with a two -dimensional area CCD detector and a high-temperature attachment. MoKα graphite -monochromated radiation (λ = 0.71073 Å) was used for data collection. The investigated samples were heated in a sealed tube as well as under normal air conditions. Data used for the determination of the crystal structure of the RbD_2PO_4 high -temperature paraelectric phase were collected at *T* = 430 K. An omega scan with $\Delta\Omega$ = 1° for each image was used for data collection. A series of 960 images in six different runs covered 89.5% of the Ewald sphere; 1764 reflections were recorded for RbD_2PO_4, which merged to give a total of 539 unique reflections. The lattice parameters were calculated from all the reflections measured. The structure of RbD_2PO_4 at 430 K was solved by the Patterson method using the SHELXS-97 program. Refine-

ment was carried out using SHELXL-97 [22]. Anisotropic thermal displacement parameters were used for all non-hydrogen atoms. The positions of hydrogen atoms were determined from difference Fourier maps and well refined. A correction for empirical absorption was applied for the observed reflections, and an extinction correction was introduced into the refinement.

3. Results and discussion

The temperature dependences of the lattice parameters for RbD_2PO_4 in the temperature range 288–537 K exhibit anomalies at 317 K and 377 K as well as structural changes at approximately 525 K (Fig. 1).

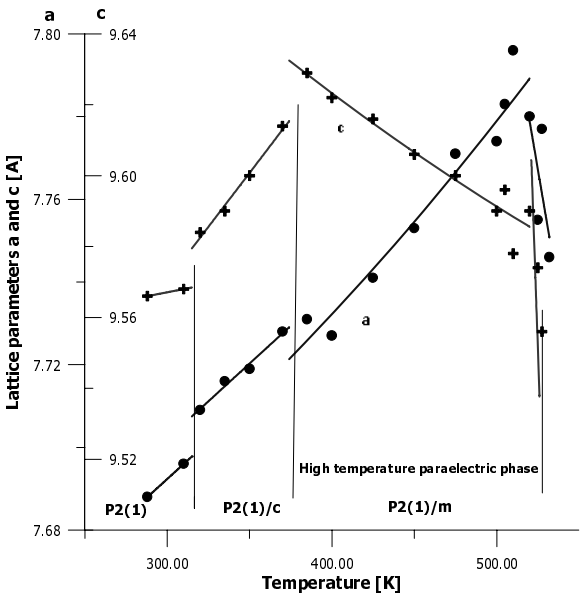

Fig. 1. The temeratpure dependences of the lattice parameters in RbD_2PO_4

The structure analyses of these crystals confirmed that the ferrielectric phase has $P2_1$ symmetry, and that the paraelectric intermediate and high-temperature phases have $P2_1/c$ and $P2_1/m$ symmetry, respectively. X-ray diffraction CCD images obtained for RbD_2PO_4 in a sealed tube above 380 K prove that the high-temperature paraelectric phase of these crystals is stable up to approximately 525 K. Figure 2a presents the X-ray CCD image of a single-crystal sample of RbD_2PO_4 heated in a sealed tube from 380 K to 525 K. The CCD image of this sample taken at 527 K (Fig. 2b) demonstrates the disappearance of the single-crystal paraelectric phase of RbD_2PO_4 and the simultaneous polycrystallisation of the sample. Additionally, X-ray powder high-temperature measurements of RbD_2PO_4, performed in a sealed tube, confirmed that the monoclinic high-temperature paraelectric

phase of the crystals is stable up to approximately 525 K. Investigations under normal air conditions have shown that the paraelectric phase of RbD_2PO_4 is stable only up to about 510 K. Above this temperature, the crystal decomposes by dehydration. The CCD image obtained for RbD_2PO_4 at 515 K has revealed that in normal air the polycrystallisation process is complete at this temperature.

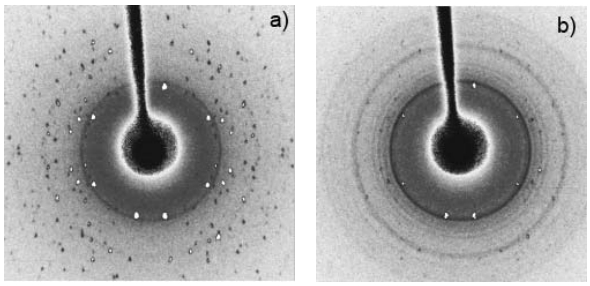

Fig. 2. X-ray diffraction CCD image of RbD_2PO_4 heated in a sealed tube at: a) 515 K, b) 527 K

Table 1. Crystal data and structure refinement for RbD_2PO_4 at 430 K

Identification code	rbd430
Empirical formula	RbD_2PO_4
Formula weight	184.47
Temperature	430(2) K
Wavelength	0.71073 Å
Crystal system space group	monoclinic $P2(1)/M$
Unit cell dimensions	a = 4.8040(10) Å b = 6.2020(12) Å c = 7.7366(15) Å β = 109.08(3) deg
Volume	217.84(7) Å^3
Z/Calculated density	2/2.812 Mg/m^3
Absorption coefficient	11.606 mm^{-1}
F(000)	172
Crystal size	0.21×0.25×0.29 mm^3
Theta range for data collection	4.31 to 28.41 deg
Index ranges	$-6 \leqslant h \leqslant 6$ $-8 \leqslant k \leqslant 4$ $-9 \leqslant l \leqslant 10$
Reflections collected/unique	1764/539 (R(int) = 0.0669)
Completeness to 2theta	28.41 89.5%
Refinement method	Full-matrix least-squares on F^2
Data/restraints/parameters	539/0/42
Goodness-of-fit on F^2	1.295
Final R indices ($I>\sigma(I)$)	R1 = 0.0334, wR2 = 0.0683
R indices (all data)	R1 = 0.0372, wR2 = 0.0694
Extinction coefficient	0.078(2)
Largest diff. peak and hole	0.519 and –0.566×10^{-3}

The crystal structure of the high-temperature paraelectric phase of RbD_2PO_4 is similar to that of CsH_2PO_4 at room temperature [14] having a monoclinic symmetry with the space group $P2_1/m$ and two chemical units in the unit cell. Nevertheless, the atomic coordinates of RbD_2PO_4 were determined independently. Crystal data and details of data collection and refinement for RbD_2PO_4 at 430 K are shown in Table 1. The final atomic coordinates and equivalent isotropic displacement parameters, with ESDs in parentheses, calculated for this crystal are presented in Table 2 (U(eq) is defined as one third of the trace of the orthogonalised U_{ij} tensor).

Table 2. Atomic coordinates ($\times 10^4$) and equivalent isotropic displacement parameters for RbD_2PO_4 at 430 K

Atom	*x*	*y*	*z*	*U*(eq)
Rb(1)	7081(1)	7500	7622(1)	48(1)
P(1)	2102(1)	2500	7452(1)	32(1)
O(1)	5054(2)	2500	9007(2)	44(1)
O(2)	2102(2)	517(2)	6307(2)	84(1)
O(3)	–197(2)	2500	8341(2)	99(1)
D(1)	6620(4)	2500	8820(3)	70(6)
D(2)	1160(6)	70(6)	5510(5)	98(12)

Figure 3 presents the projection of the atom arrangement in the unit cell of the RbD_2PO_4 crystal along the *b* axis. Some interatomic distances and angles in RbD_2PO_4 are shown in Table 3. Large values of the anisotropic displacement parameters of all oxygen atoms indicate that the structure of RbD_2PO_4 crystals is dynamically disordered. The refinement of the crystal structure revealed the isomorphism of the crystals RbD_2PO_4 at 430 K and CsH_2PO_4 at room temperature.

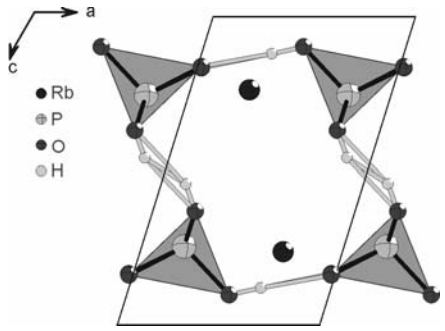

Fig. 3. The projection of the atoms arrangement in RbD_2PO_4 along the *b* axis at 430 K

Our previous powder and single-crystal diffraction investigations of CsH_2PO_4 revealed that the paraelectric phase of these crystals is stable up to approximately 504 K and that at this temperature a structural phase transition from the paraelectric phase to

the superionic phase occurs [5–8]. The superionic phases of these crystals are unstable under normal air due to dehydration.

Table 3. Selected bond lengths [Å]
and angles [deg] for RbD_2PO_4 at 430K

Rb(1)–O(2)#1	2.9437(11)	P(1)–O(3)	1.4798(16)
Rb(1)–O(3)#3	2.9898(17)	P(1)–O(2)	1.5158(11)
Rb(1)–O(1)#3	3.0988(14)	P(1)–O(2)#1	1.5158(11)
Rb(1)–O(3)#5	3.3407(7)	P(1)–O(1)	1.5304(11)
Rb(1)–O(2)#7	3.4188(14)	O(1)–D(1)	0.81(2)
Rb(1)–O(2)#4	3.4582(13)	O(2)–D(2)	0.69(3)
Rb(1)–O(1)	3.5205(8)		

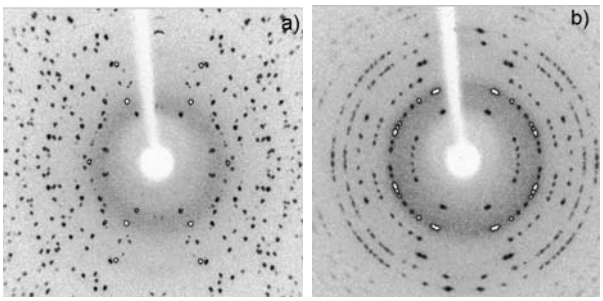

Fig. 4. Rotation CCD image of CsH_2PO_4
heated in a sealed tube at: a) 410 K, b) 509 K

X-ray rotation and oscillation CCD pictures (Fig. 4) of CsH_2PO_4 have reconfirmed that the paraelectric phase of these crystals is stable up to 504 K. At this temperature, a clear structural phase transition from the monoclinic $P2_1/m$ paraelectric phase to the

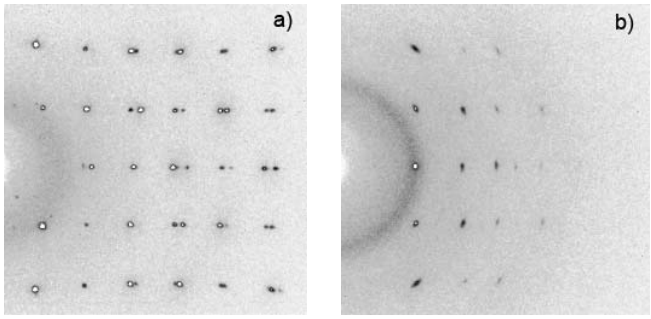

Fig. 5. Oscillation CCD picture of CsH_2PO_4 around *a*-axis
heated in a sealed tube at: a) room temperature, b) 510 K

cubic superionic phase has been observed. Figure 4a shows an X-ray rotation CCD image of a single-crystal sample of CsH_2PO_4 heated in a sealed tube from 288 K to

410 K. The rotation CCD image of this sample taken at 509 K (Fig. 4b) demonstrates an essential structural change accompanied by the superionic phase transition in the crystal.

The oscillation CCD pictures for CsH_2PO_4 around the *a*-axis taken at room temperature and 510 K are shown in Figure 4. These results unequivocally establish a cubic *Pm*-3*m* symmetry (a = 4.952(1) Å) for the superionic phase of CsH_2PO_4. Upon cooling, CsH_2PO_4 remains in the cubic phase down to a temperature of approximately 464 K. The reversible nature of the superionic transformation (with a 40° hysteresis) in CsH_2PO_4 is a strong evidence for the polymorphic character of this solid–solid transition. Detailed data of the crystal structure of the cubic superionic phases of CsH_2PO_4 and CsD_2PO_4 will be published in a following paper.

4. Conclusions

The temperature dependences of the lattice parameters of RbD_2PO_4 have revealed anomalies, which correspond to successive phase transitions at 317 K and 377 K, as well as an anomaly at approximately 525 K. The ferrielectric phase has the $P2_1$ symmetry (with $2a$, b, $2c$, Z = 8) and the paraelectric intermediate phase has $P2_1/c$ symmetry (with a, b, $2c$, Z = 4). The high-temperature paraelectric phase of RbD_2PO_4 has the $P2_1/m$ symmetry with the basis lattice parameters and Z = 2. The refinement of the crystal structure of RbD_2PO_4 at 430 K proves that the high-temperature paraelectric phase of the crystal is isomorphous with the paraelectric phase of CsH_2PO_4 at room temperature. The high-temperature paraelectric phase is stable up to approximately 525 K. At this temperature, the polycrystallisation of the single-crystal line samples and polymerisation due to their decomposition was observed.

The paraelectric phase of CsH_2PO_4 is stable up to 504 K. At this temperature, a structural phase transition from the monoclinic $P2_1/m$ paraelectric phase to the superionic phase was observed. These results undoubtedly prove the *Pm*-3*m* cubic symmetry of the superionic phase of the crystals studied. The cubic phase is stable upon cooling over the 40-degree temperature regime. The reversible nature of the superionic transformation (with a 40-degree hysteresis) in CsH_2PO_4 is a strong evidence for a polymorphic character of this solid–solid transition.

References

[1] BLINC R., O'REILLY D.E., PETERSON E.M., WILLIAMS M., J. Chem. Phys., 50 (1969), 5408.
[2] KOMUKAE M., KAWASHIMA K. OSAKA T., J. Phys. Soc. Jpn., 69 (2000), 2076.
[3] MATTAUCH S., PAULUS W., GLINNEMANN J., HEGER G., Physica B, 234–236 (1997), 40.
[4] SUMITA M., OSAKA T., MAKITA Y., J. Phys. Soc. Jpn., 50 (1981), 154.
[5] BRONOWSKA W., PIETRASZKO A., Solid State Commun., 76 (1990), 293.
[6] PRAISINGER A., MEREITER K., BRONOWSKA W., Mat. Sci. Forum, 166–169 (1994), 511.
[7] BRONOWSKA W., Adv. X-Ray Anal., 40 (1998), CD.

[8] BRONOWSKA W., J. Chem. Phys., 114 (2001), 611.
[9] SUZUKI S., ARAI K., SUMITA M., MAKITA Y., J. Phys. Soc. Jpn., 52 (1983), 2394.
[10] HAGIWARA T., ITOH K., NAKAMURA E., KOMUKAE M., MAKITA Y., Acta Cryst.C, 40 (1984), 718.
[11] OSAKA T., SUMITA M., MAKITA Y., J. Phys. Soc. Jpn., 52 (1983), 1124.
[12] MAKITA Y., SUMITA M., OSAKA T., SUZUKI S., Ferroelectrics, 39 (1981), 1017.
[13] LEVSTIK A., BLINC R., KADABA P., CIZIKOV S., LEVSTIK I., FILIPIC C., Solid State Commun., 16 (1975), 1339.
[14] UESU Y., KOBAYASHI J., Phys. Status Solidi (a), 34 (1976), M 475.
[15] BARANOV A.I., KHIZNICHENKO V.P., SHUVALOV L.A., Ferroelectrics, 100 (1989), 135.
[16] ORTIZ E., VARGAS R.A., MELLANDER B.-E., J. Chem. Phys., 110 (1999), 4847.
[17] HAILE S.M., Mater. Res. Soc. Symp. Proc., 547 (1999), 315.
[18] BOYSEN D.A., HAILE S.M., LIU H., SECCO R.A., Chem. Mater., 15 (2003), 727.
[19] LEE K.-S., J. Phys. Chem. Solids, 57 (1996), 333.
[20] PARK J.H., Phys. Rev. B, 69 (2004), 054104.
[21] OTOMO J., Solid State Ionics, 156 (2003), 357.
[22] SHELDRICK G.M., *SHELXL-97, Programs for the Solution and the Refinement of the Crystal Structures from Diffraction Data*, University of Gottingen, 1997.

Received 10 December 2004
Revised 10 September 2005